

REALIZATION OF ANALOG SIGNAL PROCESSING MODULES USING
CARBON NANOTUBE FIELD EFFECT TRANSISTORS

MUHAMMAD IDREES MASUD

UNIVERSITI TEKNOLOGI MALAYSIA

REALIZATION OF ANALOG SIGNAL PROCESSING MODULES USING
CARBON NANOTUBE FIELD EFFECT TRANSISTORS

MUHAMMAD IDREES MASUD

A thesis submitted in fulfilment of the
requirements for the award of the degree of
Doctor of Philosophy

School of Electrical Engineering
Faculty of Engineering
Universiti Teknologi Malaysia

JUNE 2022

ACKNOWLEDGEMENT

I would like to thank Allah for giving me the opportunity to undertake my studies far from home. Moreover, I thank Prof. Dr. Abu Khari Bin A'ain for his continuous guidance, tireless efforts, encouragement, and patience regarding this study. Prof. Dr. Abu Khari Bin A'ain was my first supervisor, but unfortunately he retired before my thesis submission. I am indebted for his support until the completion of my thesis.

My special gratitude is due to my supervisors Dr. Muhammad Nadzir bin Marsono, Dr. Nasir Shaikh Husin and external supervisor Dr. Iqbal A. Khan for their valuable advice and friendly help. Their critical reviews on my work and interesting suggestions have been constructive throughout this study.

My special gratitude is due to my parents and my wife for their loving support. Without their encouragement and understanding, it would have been hard for me to achieve my research objectives.

I appreciate all my friends, especially Arbab Alamgir, Dr. Ghani Ur Rehman, Yasir Ismail, Dr Waheed Younis, Dr Zubair Khalid, Dr Rashid and Dr. Touqeer Jumani, who advised and encouraged me whenever it was difficult for me.

ABSTRACT

This thesis presents the realization and performance analysis of several carbon nanotube field effect transistor (CNTFET) based analog signal processing (ASP) modules. CNTFET is predicted as a possible successor to conventional silicon complementary metal oxide semiconductor (CMOS), which has reached its scaling limits. The CMOS based ASP modules face significant challenges at deep nanoscale, resulting in severe performance degradations due to short channel effects. The main goal of this work is to realize CNTFET active building blocks (ABBs), and then to utilize these ABBs for realization of low-voltage, low-power, and high-frequency ASP modules. The proposed ABBs have low power dissipation, reduced parasitic components, and minimum number of CNTFETs. The proposed modules are active inductor (AI), first-order phase shifter, and second-order phase shifter. This research proposes a new CNTFET based grounded AI (GAI) circuit with high self-resonance frequency (SRF), wide tunable inductance range, and high quality factor. Simulation results demonstrate that the GAI offers tunable inductance from 4.4 nH to 287.4 nH with a maximum SRF of 101 GHz. It consumes very low power dissipation of 0.337 mW. In comparison to high performance available GAI circuits, the proposed GAI shows 34% reduction in power dissipation and nine times higher SRF. A high-frequency low-noise amplifier (LNA) circuit is also designed by utilizing the proposed GAI to showcase its application. The simulation result shows high frequency bandwidth of 17.5 GHz to 57 GHz, 15.9 dB maximum voltage gain, better than -10 dB input matching, and less than 3 dB noise figure. This research also proposes a compact wideband first-order phase shifter (FOPS) and active-only FOPS (AOFOPS). Simulation results demonstrate the FOPS has a tunable pole frequency range between 1.913 GHz and 40.2 GHz, input and output voltage noises of $4.402 \text{ nV}/\sqrt{\text{Hz}}$ and $4.414 \text{ nV}/\sqrt{\text{Hz}}$ respectively, and power dissipation of 0.4862 mW. The AOFOPS circuit also offers a wide tunable range of pole frequency between 34.2 GHz to 56.4 GHz with input noise and output noise of $6.822 \text{ nV}/\sqrt{\text{Hz}}$ and $6.761 \text{ nV}/\sqrt{\text{Hz}}$ respectively, and power dissipation of only 0.0338 mW. The AOFOPS dissipates 12.40 times less power in comparison to state-of-art FOPS circuits. This work also proposes active-only second-order phase shifter. The proposed circuit provides a tunable pole frequency between 16.2 GHz to 42.5 GHz, with input and output noises of $21.698 \text{ nV}/\sqrt{\text{Hz}}$ and $21.593 \text{ nV}/\sqrt{\text{Hz}}$ respectively, while consuming 0.2256 mW power. All circuit performances are verified through HSPICE simulation by utilizing the Stanford CNTFET model at 16 nm technology node with supply voltage of 0.7 V.

ABSTRAK

Tesis ini membentangkan realisasi dan analisis prestasi beberapa modul pemrosesan isyarat analog (ASP) berasaskan transistor kesan medan nanotub karbon (CNTFET). CNTFET diramalkan sebagai pengganti kepada semikonduktor oksida logam pelengkap (CMOS) silikon lazim, yang sudah mencapai had penskalaannya. Modul ASP CMOS menghadapi cabaran besar pada skala-nano dalam, yang menyebabkan kemerosotan prestasi yang teruk kerana kesan saluran pendek. Tujuan utama kerja ini adalah untuk merealisasi blok binaan aktif (ABB), dan kemudiannya digunakan untuk merealisasi modul ASP voltan-rendah dan kuasa-rendah yang berfrekuensi tinggi. ABB yang dicadangkan mempunyai pelepasan kuasa yang rendah, kebolehtalaan yang tinggi, pengurangan komponen parasit, dan menggunakan bilangan CNTFET yang minimum. Modul yang dicadangkan adalah induktor aktif (AI), penganjak fasa tertib-pertama, dan penganjak fasa tertib-kedua. Penyelidikan ini mencadangkan litar AI terbumi (GAI) CNTFET yang baharu yang mempunyai ciri-ciri frekuensi swaresonans (SRF) yang tinggi, kearuhan yang boleh ditala dalam julat yang lebar, dan faktor kualiti yang tinggi. Hasil simulasi menunjukkan bahawa litar GAI menawarkan aruhan boleh ditala dari 4.4 nH hingga 287.4 nH dengan SRF maksimum 101 GHz. Ia melepaskan kuasa yang sangat rendah iaitu 0.337 mW. Berbandingkan dengan litar GAI berprestasi tinggi sedia ada, GAI yang dicadangkan menunjukkan pengurangan pelepasan kuasa sebanyak 34% dan peningkatan SRF sembilan kali lebih tinggi. Litar penguat rendah-hingar (LNA) berfrekuensi tinggi juga direka bentuk berdasarkan GAI yang dicadangkan untuk menunjukkan pengaplikasiannya. Hasil simulasi menunjukkan lebar jalur frekuensi yang tinggi iaitu 17.5 GHz hingga 57 GHz, gandaan voltan maksimum 15.9 dB, padanan input melebihi -10 dB, dan angka hingar kurang dari 3 dB. Penyelidikan ini juga mencadangkan penganjak fasa tertib-pertama (FOPS) dan FOPS hanya-aktif (AOFOPS). Hasil simulasi FOPS menunjukkan julat frekuensi kutub yang boleh diatur antara 1.913 GHz dan 40.2 GHz, hingar voltan masukan dan voltan keluaran masing-masing $4.402 \text{ nV}/\sqrt{\text{Hz}}$ dan $4.414 \text{ nV}/\sqrt{\text{Hz}}$, dan pelepasan kuasa 0.4862 mW. Litar AOFOPS ini juga menawarkan frekuensi kutub yang dapat ditala dengan luas antara 34.2 GHz hingga 56.4 GHz dengan hingar masukan dan hingar keluaran masing-masing $6.822 \text{ nV}/\sqrt{\text{Hz}}$ dan $6.761 \text{ nV}/\sqrt{\text{Hz}}$ dan pelepasan kuasa hanya 0.0338 mW. Litar AOFOPS yang dicadangkan dapat mengurangkan pelepasan kuasa sebanyak 12.40 kali berbanding litar FOPS terkini. Penyelidikan ini juga mencadangkan penganjak fasa hanya-aktif tertib-kedua. Litar yang dicadangkan menyediakan frekuensi kutub yang dapat ditala antara 16.2 GHz hingga 42.5 GHz, dengan hingar masukan dan hingar keluaran masing-masing $21.698 \text{ nV}/\sqrt{\text{Hz}}$ dan $21.593 \text{ nV}/\sqrt{\text{Hz}}$, dan penggunaan kuasa 0.2256 mW. Semua prestasi litar disahkan melalui simulasi HSPICE yang menggunakan model CNTFET Stanford pada nod teknologi 16 nm dengan bekalan kuasa 0.7 V.

TABLE OF CONTENTS

	TITLE	PAGE
	DECLARATION	iii
	DEDICATION	iv
	ACKNOWLEDGEMENT	v
	ABSTRACT	vi
	ABSTRAK	vii
	TABLE OF CONTENTS	viii
	LIST OF TABLES	xi
	LIST OF FIGURES	xii
	LIST OF ABBREVIATIONS	xvii
	LIST OF SYMBOLS	xviii
CHAPTER 1	INTRODUCTION	1
1.1	Background	1
1.2	Problem Statement	4
1.3	Research Objectives	6
1.4	Scope and Limitations	6
1.5	Research Contributions	7
1.6	Thesis Organization	8
CHAPTER 2	LITERATURE REVIEW	11
2.1	Introduction	11
2.2	Active Inductor	11
2.2.1	Gyrator-C Active Inductor	12
2.2.2	Grounded Active Inductor Circuit Topologies	15
2.3	Phase Shifter	22
2.3.1	First Order Phase Shifter	25
2.3.2	Second Order Phase Shifter	31
2.4	Carbon Nanotube Field Effect Transistor	36

2.5	Summary	40
CHAPTER 3	METHODOLOGY	41
3.1	Introduction	41
3.2	Research Framework	42
3.3	Realization of ABB	44
3.4	Realization of ASP Modules	46
3.5	Device Model	48
3.6	Summary	50
CHAPTER 4	GROUNDING ACTIVE INDUCTOR	51
4.1	Introduction	51
4.2	CNTFET Based Active Building Blocks	52
4.2.1	CNTFET Based Inverting Voltage Buffer	53
4.2.2	CNTFET Based Transconductance Elements	59
4.3	PTE and NTE Based GAI Circuit Topology	63
4.4	GAI Design and Verification	70
4.5	LNA Design Using Proposed CNTFET GAI	78
4.5.1	Circuit Description	79
4.5.2	LNA Simulations Results	81
4.6	GAI Comparative Study	85
4.7	Summary	86
CHAPTER 5	IVB BASED FIRST ORDER PHASE SHIFTERS	87
5.1	Introduction	87
5.2	IVB Based FOPS	88
5.2.1	FOPS Circuit Description	88
5.2.2	FOPS Design and Verification	92
5.3	IVB Based AOFOPS	101
5.3.1	AOSOPS Circuit Description	102
5.3.2	AOSOPS Design and Verification	105
5.4	FOPS Comparative Study	110
5.5	Summary	110

CHAPTER 6	ACTIVE ONLY SECOND ORDER PHASE SHIFTER	113
6.1	Introduction	113
6.2	AOSOPS Circuit Description	114
6.3	AOSOPS Design and Verification	120
6.4	AOSOPS Comparative Study	129
6.5	Summary	130
CHAPTER 7	CONCLUSION	131
7.1	Research Summary	131
7.2	Future Work	132
REFERENCES		135
LIST OF PUBLICATIONS		147

LIST OF TABLES

TABLE NO.	TITLE	PAGE
Table 2.1	Summary of related GAI circuits	23
Table 2.2	Summary of related FOPS circuits	30
Table 2.3	Summary of related SOPS circuits	35
Table 3.1	The CNTFET parameters	49
Table 4.1	Design parameter values for dual negative feedback LNA	82
Table 4.2	Design parameter values for GAI of Figure 4.18	82
Table 4.3	GAI performance comparison	86
Table 5.1	Comparison with reported FOPS topologies	111
Table 6.1	Comparison with reported SOPS topologies	129

LIST OF FIGURES

FIGURE NO.	TITLE	PAGE
Figure 1.1	Beamforming scheme [17]	3
Figure 2.1	Gyrator-C GAI [24]	12
Figure 2.2	Bode plot of gyrator-C AI input impedance (Z_{in}) [25]	14
Figure 2.3	GAI topologies reported in [35] (a) Basic flipped-AI (b) Cascoded flipped-AI (c) Small signal equivalent circuit of cascoded flipped-AI	16
Figure 2.4	GAI reported in [36]	17
Figure 2.5	GAI reported in [37]	18
Figure 2.6	GAI reported in [43]	19
Figure 2.7	GAI reported in [45]	21
Figure 2.8	GAI reported in [46]	22
Figure 2.9	FOPS reported in [70]	26
Figure 2.10	FOPS reported in [71]	26
Figure 2.11	FOPS reported in [72]	27
Figure 2.12	FOPS reported in [73]	28
Figure 2.13	FOPS reported in [79]	28
Figure 2.14	FOPS reported in [80]	29
Figure 2.15	SOPS reported in [48]	32
Figure 2.16	SOPS reported in [49]	32
Figure 2.17	SOPS reported in [85] (a) Topology-1 (b) Topology-2	33
Figure 2.18	SOPS reported in [86]	34
Figure 2.19	CNT structure (a) Single-wall (a) Multi-wall	36
Figure 2.20	CNTFET structure	37
Figure 2.21	A graphene sheet rolled to demonstrate formation of various types of single-wall CNTs [88]	38
Figure 3.1	Research framework	43
Figure 3.2	Roadmap to realization of ABB	45

Figure 3.3	Roadmap to realization of ASP module	47
Figure 4.1	IVB (a) CNTFET implementation (b) Symbol	54
Figure 4.2	IVB non-ideal parasitic model	54
Figure 4.3	Frequency response of IVB output impedance	55
Figure 4.4	Impact of variation of N_T on R_o	56
Figure 4.5	Impact of variation of N_T on C_i and C_o	56
Figure 4.6	Impact of variation of N_T on power dissipation	56
Figure 4.7	Impact of variation of D_T on R_o	57
Figure 4.8	Impact of variation of D_T on power dissipation	57
Figure 4.9	Impact of variation of S_T on R_o	58
Figure 4.10	Impact of variation of S_T on power dissipation	58
Figure 4.11	NTE (a) CNTFET implementation (b) Symbol	59
Figure 4.12	NTE non-ideal parasitic model	59
Figure 4.13	PTE (a) CNTFET implementation (b) Symbol	60
Figure 4.14	PTE non-ideal parasitic model	60
Figure 4.15	Frequency response of transconductance of PTE and NTE with different N_{TS}	61
Figure 4.16	Impact of variation of N_T on g_m	62
Figure 4.17	Impact of variation of N_T on power dissipation	63
Figure 4.18	Proposed CNTFET based GAI topology	63
Figure 4.19	Varactor transistor level realization with its symbol	64
Figure 4.20	Equivalent small signal model at node V_1	64
Figure 4.21	Equivalent small signal model at node V_2	64
Figure 4.22	Equivalent small signal model at node V_j	65
Figure 4.23	RLC equivalent circuit for proposed CNTFET based GAI	69
Figure 4.24	Frequency response of Z_{in} magnitude at $V_{tune} = -0.60 V$	72
Figure 4.25	Frequency response of Z_{in} phase at $V_{tune} = -0.60 V$	72
Figure 4.26	Frequency response of GAI inductance (for positive values only)	73

Figure 4.27	Frequency response of GAI QF at $V_{tune} = -0.60 V$	74
Figure 4.28	Impact of variation of k on inductance L	74
Figure 4.29	Impact of variation of k on SRF	75
Figure 4.30	Frequency response of Z_{in} magnitude at different values of V_{tune}	76
Figure 4.31	Frequency response of GAI inductance at different values of V_{tune} (for positive values only)	76
Figure 4.32	Variation of GAI inductance versus V_{tune}	77
Figure 4.33	Variation of GAI SRF versus V_{tune}	77
Figure 4.34	Dual negative feedback LNA [113]	79
Figure 4.35	Dual negative feedback LNA	80
Figure 4.36	GAI based LNA gain versus frequency	83
Figure 4.37	GAI based LNA NF versus frequency	83
Figure 4.38	S_{11} versus frequency	84
Figure 4.39	S_{22} versus frequency	84
Figure 4.40	S_{12} versus frequency	85
Figure 5.1	CNTFET-C FOPS topology-1	89
Figure 5.2	CNTFET-C FOPS topology-2	91
Figure 5.3	Calculated and simulated frequency response of gain of the proposed FOPS topology-1	93
Figure 5.4	Calculated and simulated frequency response of phase angle of the proposed FOPS topology-1	93
Figure 5.5	Frequency response of input output noise of the proposed FOPS topology-1	94
Figure 5.6	Output resistance R_{OT} variations with different values of V_C	95
Figure 5.7	Calculated and simulated frequency response of gain of the proposed FOPS topology-2	95
Figure 5.8	Calculated and simulated frequency response of phase angle of the proposed FOPS topology-2	96
Figure 5.9	Frequency response of input output noise of the proposed FOPS topology-2	96

Figure 5.10	Frequency response of gain of the FOPS topology-2 at different V_C	97
Figure 5.11	Frequency response of phase angle of the FOPS topology-2 at different V_C	97
Figure 5.12	Monte Carlo simulations of FOPS topology-2 for gain at $V_C = 0.40 V$	98
Figure 5.13	Monte Carlo simulations of FOPS topology-2 for phase at $V_C = 0.40 V$	99
Figure 5.14	Frequency response of FOPS topology-2 gain with different supply voltages V_{DD} at $V_C = 0.40 V$	99
Figure 5.15	Frequency response of FOPS topology-2 phase with different supply voltages V_{DD} at $V_C = 0.40 V$	100
Figure 5.16	Frequency response of FOPS topology-2 gain with different temperatures at $V_C = 0.40 V$	100
Figure 5.17	Frequency response of FOPS topology-2 phase with different temperatures at $V_C = 0.40 V$	101
Figure 5.18	CNTFET-AOFOPS transistor level realization	102
Figure 5.19	CNTFET based varactor (a) Transistor level realization (b) Symbol	102
Figure 5.20	C-V characteristics of varactor with different N_T	105
Figure 5.21	Calculated and simulated frequency response of gain of the AOFOPS at $V_{tune} = -0.32 V$	106
Figure 5.22	Calculated and simulated frequency response of phase of the AOFOPS at $V_{tune} = -0.32 V$	106
Figure 5.23	Frequency response of input and output noises of AOFOPS at $V_{tune} = -0.32 V$	107
Figure 5.24	Monte Carlo simulations of AOFOPS for gain at $V_{tune} = -0.32 V$	108
Figure 5.25	Monte Carlo simulations of AOFOPS for phase at $V_{tune} = -0.32 V$	108
Figure 5.26	Frequency response of gain of the AOFOPS for different control voltages V_{tune}	109
Figure 5.27	Frequency response of phase of the AOFOPS for different control voltages V_{tune}	109
Figure 6.1	CNTFET based AOSOPS	114

Figure 6.2	CNTFET based VCR (a) Transistor level realization (b) Symbol	115
Figure 6.3	CNTFET based AOSOPS with NTE and PTE parasitics	117
Figure 6.4	Simplified circuit for AOSOPS with parasitics	118
Figure 6.5	Frequency response of PTE and NTE transconductance with $N_T=2$	120
Figure 6.6	CV characteristics of varactor with $N_T=150$	122
Figure 6.7	Calculated (obtained from Equation 6.17) and simulated frequency response of gain of the AOSOPS at $V_{tune}=-0.308 V$ and $V_Q=0.68 V$	122
Figure 6.8	Calculated (obtained from Equation 6.17) and simulated frequency response of phase of the AOSOPS at $V_{tune}=-0.308 V$ and $V_Q=0.68 V$	123
Figure 6.9	Frequency response of gain of the AOSOPS with $V_Q=0.68 V$ and different values of V_{tune}	124
Figure 6.10	Frequency response of phase of the AOSOPS with $V_Q=0.68 V$ and different values of V_{tune}	124
Figure 6.11	Frequency response of input output noise of AOSOPS at $V_{tune}=-0.40 V$ and $V_Q=0.68 V$	125
Figure 6.12	Monte Carlo simulations of AOSOPS for gain at $V_{tune}=-0.40 V$ and $V_Q=0.68 V$	126
Figure 6.13	Monte Carlo simulations of AOSOPS for phase at $V_{tune}=-0.40 V$ and $V_Q=0.68 V$	126
Figure 6.14	Frequency response of AOSOPS gain with different supply voltages V_{DD} at $V_{tune}=-0.40 V$ and $V_Q=0.68 V$	127
Figure 6.15	Frequency response of AOSOPS phase with different supply voltages V_{DD} at $V_{tune}=-0.40 V$ and $V_Q=0.68 V$	127
Figure 6.16	Frequency response of AOSOPS gain with different temperatures at $V_{tune}=-0.40 V$ and $V_Q=0.68 V$	128
Figure 6.17	Frequency response of AOSOPS phase with different temperatures at $V_{tune}=-0.40 V$ and $V_Q=0.68 V$	128

LIST OF ABBREVIATIONS

ABBs	-	Active Building Blocks
AI	-	Active Inductor
AOFOPS	-	Active Only First Order Phase Shifter
AOSOPS	-	Active Only Second Order Phase Shifter
ASP	-	Analog Signal Processing
CG	-	Common Gate
CMOS	-	Complementary Metal Oxide Semiconductor
CNTFET	-	Carbon Nanotube Field Effect Transistor
CS	-	Common Source
DSP	-	Digital Signal processing
FOPS	-	First Order Phase Shifter
GAI	-	Grounded Active Inductor
GCS	-	Graphite Cylindrical Sheets
Gyrator-C	-	Gyrator-Capacitance
IC	-	Integrated Circuit
IVB	-	Inverting Voltage Buffer
LNA	-	Low Noise Amplifier
NF	-	Noise Figure
NTE	-	Negative Transconductance Element
OTA	-	Operational Transconductance Amplifier
PTE	-	Positive Transconductance Element
QF	-	Quality Factor
SRF	-	Self Resonance Frequency
VCO	-	Voltage Controlled Oscillator
VCR	-	Voltage Controlled Resistor

LIST OF SYMBOLS

π	-	Pi
Ω	-	Ohm
ω	-	Pole frequency
\mathcal{U}	-	Mho
C_{gs}	-	Gate to source capacitance
dB	-	Decibel
D_T	-	Diameter of CNT
g_{ds}	-	Output conductance
GHz	-	Gigahertz
g_m	-	Transconductance
MHz	-	Megahertz
nH	-	Nanohenry
nm	-	Nanometer
N_T	-	Number of CNTs
S_T	-	CNT pitch

CHAPTER 1

INTRODUCTION

1.1 Background

For future data processing and high speed telecommunication solutions, analog signal processing (ASP) techniques are considered as a promising alternative to digital signal processing (DSP) techniques, as analog devices outperform their digital-counterparts in terms of power dissipation, cost and the maximum achievable bandwidth [1]. Thus, ASP modules are considered as unavoidable and significant component of system on chip. They play vital role in a variety of high-performance applications such as a low noise amplifier (LNA) [2], continuous time filters [3], voltage controlled oscillators (VCOs) [4] and phase shifters [5].

Due to persistent focus on Moore's law transistor scaling and continuous technological advancements, complementary metal oxide semiconductor (CMOS) based ASP modules are prominent in the last four decades. However, reduction of channel length below 32 nm complicates designing for present CMOS technologies due to short channel effects, increased leakage current, decreased gate control and sensitivity to process variations in integrated circuit (IC) manufacturing [6]. Therefore, it is extremely imperative for IC industry to explore new materials as well as devices that equally works well for more-than-Moore technologies and beyond CMOS as coined by International Roadmap for Devices and Systems (IRDS) [7, 8]. The latest report by IRDS for 2021 [8] predicts that CNTFET is a possible replacement for CMOS technology from 2025 onwards.

To find replacements for CMOS technology, many devices and techniques are introduced and evaluated by researchers such as double gate field effect transistor (FET), single electron transistor, fin FET and carbon nanotube FET (CNTFET) [9]. Among these solutions, CNTFETs are considered front runners for further continuation of scaling down the feature length and extension of the saturated Moore's law [8, 10, 11]. Since the operational principle and the device structure of CNTFET is similar to CMOS device, it is possible that CNTFET can use efficiently the existing CMOS design infrastructure and CMOS fabrication process [12].

Since CNTFET introduction as an alternative for CMOS technology, circuit level realization in the digital domain has been demonstrated by many researchers; however, limited works have been done on the design and analysis of CNTFET based ASP modules [13]. This unexplored territory of CNTFET based ASP modules opens a new research area, which needs to be explored for the future demands of ASP applications in nanometer regime. For IC designers, the cost and integration of ASP chip for smaller chip area, low power dissipation and larger bandwidth are emerging issues. The recent push towards 5G/6G communication systems and other similar applications further aggravate these design challenges [14].

Inductors are important components that play a key role in the design of these ASP modules. Majority of ASP modules utilizes on-chip passive spiral inductors. However, spiral inductor faces several disadvantages like larger chip area, low and fixed inductance, low self-resonance frequency (SRF), low quality factor (QF) and incompatibility with low-cost standard semiconductor process [15, 16]. In consequence, the use of active inductors (AIs) instead of passive spiral inductors improve the design of ASP modules by reducing the cost and size of chips [16]. Moreover, the tunability of AI further improves the design of these modules and helps designers to adapt specifications for different ASP applications. However, the design of AI with low power dissipation, large inductive bandwidth, large inductance magnitude and high QF is a challenging task. If these design challenges are solved, the applications of AI will be expanded in the development of several other ASP modules such as VCO, LNA, power dividers and frequency selective filters.

State-of-the-art continuous time signal processing applications utilize one or more types of ASP module, as it is not possible to use a single type of module to cater for the needs of different systems with diversified inputs/outputs. Figure 1.1 demonstrates an example of beamforming scheme where different types of ASP module are utilized for their intended goals [17]. Like AI, phase shifter is another important multipurpose ASP module that functions as a fundamental building block of many analog signal processors [18]. It finds applications in the realization of various high-Q frequency selective circuits, beamforming, radar systems as well as oscillators [19, 20]. Design of area efficient, low voltage, low power phase shifter with tunable pole frequency is another challenging task.

ASP modules are mostly based on different active building blocks (ABBs) that best suit the desired applications. Design of AI and phase shifter for broadband high frequency applications is a very challenging task, especially when dealing with CNTFET based ABBs. For high frequency applications, ABBs are very sensitive to device parasitics and their power dissipation may affect the performance of desired ASP module [21]. Thus realization/selection of an efficient active device that contributes less parasitics and low power dissipation to the ASP module is a crucial requirement.

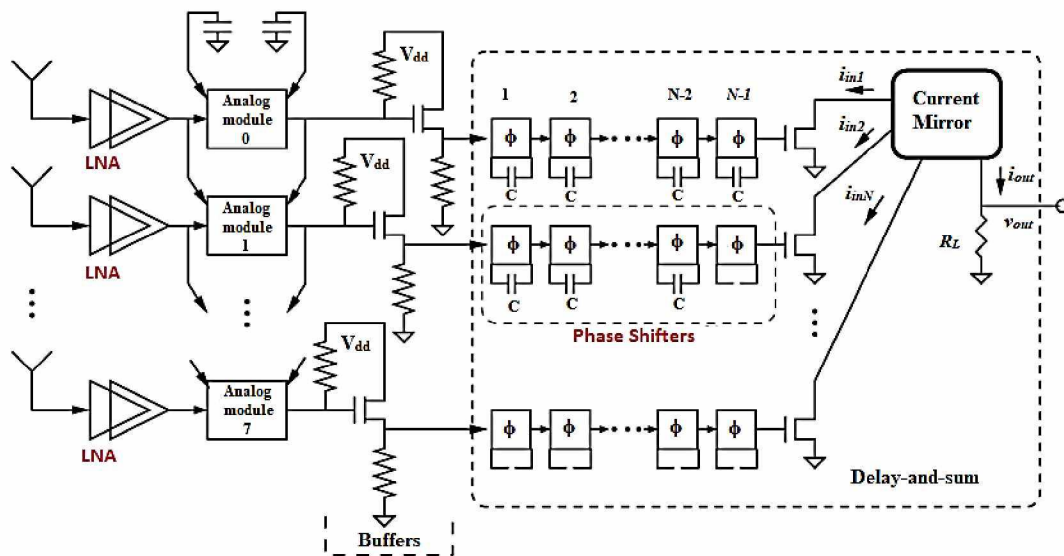


Figure 1.1 Beamforming scheme [17]

The system design of CNTFET based ASP modules for multipurpose high frequency broadband applications must provide desired functionality with improved performance, reduced active and passive devices, and minimize parasitic effect by choosing suitable and efficient topology.

1.2 Problem Statement

Designing low voltage, low power CNTFET based ASP modules for broadband high frequency applications is not a straightforward task, as performance of an ASP module is very much dependent on high frequency parasitic effects [21, 22]. The first crucial requirement in the design of such ASP module is to explore different application specific ABBs, which provide low power consumption, lower parasitic design effects, large signal bandwidth and arithmetic operation capability.

In design of ASP modules for high frequency applications, non-ideal port parasitics of used ABBs ultimately increase the design complexity of the modules and also impose serious frequency limitations on the operation and performance [22, 16]. These limitations can be minimized by realization of efficient circuit topology during the design phase of specific ASP module. Moreover, selection of the most appropriate CNTFET design parameters (inter CNT pitch, CNT diameter/chirality vector and number of CNTs) is another critical task of the design phase [6, 10-12].

ABB based AI with high inductance, high SRF, high tunability within an acceptable QF are the most challenging tasks for high frequency broadband applications [23]. Tunability of AI is an important feature that enables designers to adapt specification of different broadband applications. This desirable feature helps in the frequency band selection of filters, VCOs and so many other applications [5, 15, 24-31]. Many recently published high QF AI topologies do not have tunability feature [32-34]. Thus, these AIs are not suitable for broadband applications and can be used only for specific applications with fixed inductance and QF value. High inductance AI with acceptable QF is another important requirement [25]. In RF

circuits such as LNA, high inductance is necessary for high gain as LNA gain is dependent on magnitude of output inductance [23].

Although most AI circuit topologies presented to date are compact and achieve acceptably larger QF than its spiral counterpart, their application in low voltage, low power broadband ASP modules has been limited because of their narrow inductive bandwidth [35-46]. As a result, to the best of our knowledge, no AI circuit topology has been utilized for a high frequency (> 11 GHz) and wideband (> 7 GHz bandwidth) ASP module [47]. This comparatively narrow inductive bandwidth ultimately excludes AI for the design of broadband high frequency ASP modules.

For flexibility, the pole frequency of a phase shifter should be widely tunable. Tunability of pole frequency enables a phase shifter to be used in broadband applications [48, 49]. Low power dissipation of a phase shifter can be obtained by minimizing number of active and passive devices [50]. Moreover, the ABB power dissipation will be added to the total phase shifter power consumption, so use of ABB with less power dissipation is needed.

Based on AI and phase shifter examples, in summary, the design challenges involve low power dissipation, high tunability, minimization of parasitic components (which degrade high frequency performance) and selection of appropriate CNTFET design parameters (inter CNT pitch, CNT diameter/chirality vector and number of CNTs). In addition, high SRF and highly tunable AI with acceptable QF are other research challenges.

1.3 Research Objectives

The objectives of this research work are:

- i. To design CNTFET based ABBs suitable for the realization of low power and high frequency ASP modules. These ABBs are inverting voltage buffer (IVB), negative transconductance element (NTE) and positive transconductance element (PTE). The ASP modules to be realized using designed ABBs are AI, first order phase shifter (FOPS) and second order phase shifter (SOPS). The CNTFET ABBs are targeted to operate up to 100 GHz and with less than 1 mW power dissipation.
- ii. To design CNTFET based AI circuit topology for high frequency broadband applications. The AI circuit will be realized using the designed ABBs to achieve high QF, high tunable inductance, high SRF and low power dissipation. The target performance is for the AI circuit to be inductive up to 100 GHz with a power dissipation less than 1 mW.
- iii. To design CNTFET based FOPS and SOPS topologies for high frequency applications. The phase shifter circuits will be realized using the designed ABBs to achieve large tunable pole frequency with less than 1 mW power dissipation.

1.4 Scope and Limitations

The major scope and limitations of this research work are as follows:

- i. This study is mainly concerned with the design of ASP modules for high frequency broadband applications using CNTFET ABBs. These modules only include CNTFET based AI and phase shifters.
- ii. HSPICE simulation tool will be used for design and analysis of ABB and the ASP modules. This work will be purely based on simulation at transistor level due to the unavailability of CNTFET circuit fabrication facility.

- iii. Stanford CNTFET model at 16 nm technology node will be utilized for design of AI and phase shifter circuits.

1.5 Research Contributions

Contributions of this thesis are listed as follows:

- i. The first contribution of this work is the proposal for a new compact CNTFET based ABB known as PTE. Circuit analysis shows that the proposed ABB is a suitable candidate for low voltage, low power broadband applications, with voltage supply as low as 0.7 V and power dissipation in the μW range.
- ii. The second contribution of this research work is proposal for CNTFET based grounded AI (GAI) circuit. The GAI was designed and simulated using 16 nm CNTFET technology node using HSPICE. Simulation results demonstrate that realized GAI circuit offers high tunable inductance from 4.4 nH to 287.4 nH with a maximum SRF of 101 GHz. It offers low power dissipation of 0.337 mW. Tunability of the GAI has been achieved by utilizing CNTFET varactor. A broadband LNA circuit was also designed and simulated by utilizing the proposed GAI topology. The simulation result shows very high frequency bandwidth of 17.5 GHz to 57 GHz and dissipates 6.961 mW from 0.7 V supply. Moreover, the GAI based LNA provides a 15.9 dB maximum gain. In addition, better than -10 dB input matching and less than 3 dB noise figure (NF) over the entire bandwidth is observed.
- iii. The third contribution of this research is the proposal for a compact wideband FOPS using CNTFET based Inverting Voltage Buffer (IVB) and Voltage Controlled Resistor (VCR). Simulation results demonstrate a tunable pole frequency range between 1.913 GHz and 40.2 GHz with input and output voltage noises of $4.402 \text{ nV}/\sqrt{\text{Hz}}$ and $4.414 \text{ nV}/\sqrt{\text{Hz}}$ respectively, and power dissipation of 0.4862 mW.

- iv. The fourth contribution of this research is the design of an active only first order phase shifter (AOFOPS) using IVB and CNTFET varactor. The active only circuit topology offers a wide tunable range of pole frequency between 34.2 GHz to 56.4 GHz. Simulation results show that the equivalent input noise and output noise for the realized all active phase shifter at a designed pole frequency of 49.26 GHz are $6.822 \text{ nV}/\sqrt{\text{Hz}}$ and $6.761 \text{ nV}/\sqrt{\text{Hz}}$ respectively, while it dissipates 0.0338 mW.
- v. The fifth contribution of this research is the design of an active only second order phase shifter (AOSOPS) by utilizing two negative transconductance elements (NTE), one PTE, two varactors and one VCR. The AOSOPS topology provides a tunable pole frequency between 16.2 GHz to 42.5 GHz with input and output noise of $21.698 \text{ nV}/\sqrt{\text{Hz}}$ and $21.593 \text{ nV}/\sqrt{\text{Hz}}$ respectively. The power dissipation of AOSOPS is 0.2256 mW.

1.6 Thesis Organization

This dissertation is organized into seven chapters. Chapter 1 discusses the background, problem statement, objectives and scope of this research work. Moreover, this chapter also highlights the contributions of this research work.

Chapter 2 of this dissertation provides a summary of advanced AI and phase shifter circuit topologies available in the open literature. The performance of these available ASP modules is discussed and investigated thoroughly.

Chapter 3 of this thesis discusses the methodology adopted in this research work. Moreover, the flow of the complete design process steps is discussed thoroughly for the realization of CNTFET ABBs and ASP modules.

Chapter 4 introduces the proposed GAI circuit. The GAI equivalent parasitic model will be explained in this chapter. Also, equations for inductance and QF will be analyzed. Simulation results of the GAI topology will also be explained thoroughly. Moreover, the application of the proposed GAI in the design of broadband LNA will be demonstrated.

Chapter 5 introduces the proposed FOPS topologies. The realized circuit description, analysis and simulation results will be explained in this chapter. Moreover, a brief comparison of the proposed circuits with other available FOPS topologies in the open literature will be discussed.

Chapter 6 introduces the AOSOPS circuit. The proposed AOSOPS circuit design and simulation results are discussed in this chapter. In addition, a comparison study with other SOPS circuits is conducted and discussed. Lastly, the conclusion and recommendations for further research is presented in Chapter 7.

REFERENCES

- [1] de França Ferreira, João Alberto, Emilie Avignon-Meseldzija, Pietro Maris Ferreira, Julien Sarrazin, and Philippe Bénabès. (2020). "Design of integrated all-pass filters with linear group delay for analog signal processing applications." *International Journal of Circuit Theory and Applications*, 48(5), 658-673.
- [2] Yaghouti, Behnam Dorostkar, and Javad Yavandhasani. (2021). "A high linearity low power low-noise amplifier designed for ultra-wide-band receivers." *Analog Integrated Circuits and Signal Processing*, 107, 109-120.
- [3] Yesil, Abdullah, Erkan Yuce, and Shahram Minaei. (2020), "MOSFET-C-based grounded active inductors with electronically tunable properties." *International Journal of RF and Microwave Computer-Aided Engineering*, 30(8), 1-13, e22274.
- [4] Kumar, Nitin, and Manoj Kumar. (2021). "Low Power CMOS Differential Ring VCO Designs using Dual Delay Stages in 0.13 μm Technology for Wireless Applications." *Microelectronics Journal*, 111, 1-12, 105025.
- [5] Aghazadeh, Seyed Rasoul, Herminio Martínez García, Alireza Saberhari, and Eduardo José Alarcón Cot. (2018). "Tunable wide-band second-order all-pass filter-based time delay cell using active inductor." *32nd Conference on Design of Circuits and Integrated Systems, (DCIS). IEEE*. 1-5.
- [6] Loan, Sajad A., M. Nizamuddin, Abdul R. Alamoud, and Shuja A. Abbasi. (2015). "Design and comparative analysis of high performance carbon nanotube-based operational transconductance amplifiers." *Nano* 10(03), 1-11, 1550039.
- [7] Obite, Felix, Geoffrey Ijeomah, and Joseph Stephen Bassi. (2019) "Carbon nanotube field effect transistors: toward future nanoscale electronics." *International Journal of Computers and Applications*, 41(2), 149-164.
- [8] IRDS 2021 edition, Available at: <https://irds.ieee.org/editions/2021/beyond-cmos>.

- [9] Cen, Mingcan, Shuxiang Song, and Chaobo Cai. (2017). "A high performance CNFET-based operational transconductance amplifier and its applications." *Analog Integrated Circuits and Signal Processing*, 91(3), 463-472.
- [10] Imran, Ale, Mohd Hasan, Aminul Islam, and Shuja Ahmad Abbasi. (2012). "Optimized design of a 32-nm CNFET-based low-power ultrawideband CCII." *IEEE transactions on Nanotechnology*, 11(6), 1100-1109.
- [11] Jogad, Seema, Sajad A. Loan, Neelofer Afzal, and Abdullah G. Alharbi. (2021). "CNTFET based class AB current conveyor II: Design, analysis and waveform generator applications." *International Journal of Numerical Modelling: Electronic Networks, Devices and Fields*, 34(1), 1-15, e2783.
- [12] Nizamuddin, M., Sajad A. Loan, Abdul R. Alamoud, and Shuja A. Abbassi. (2015). "Design, simulation and comparative analysis of CNT based cascode operational transconductance amplifiers." *Nanotechnology*, 26(39), 1-13, 395201.
- [13] Prakash, P., K. Mohana Sundaram, and M. Anto Bennet. (2018). "A review on carbon nanotube field effect transistors (CNTFETs) for ultra-low power applications." *Renewable and Sustainable Energy Reviews*, 89, 194-203.
- [14] Tsai, Ching-Han, Chun-Yi Lin, Ching-Piao Liang, Shyh-Jong Chung, and Jenn-Hwan Tarng. (2021). "Switched Low-Noise Amplifier Using Gyrator-Based Matching Network for TD-LTE/LTE-U/Mid-Band 5G and WLAN Applications." *Applied Sciences*, 11(4), 1-13, 1477.
- [15] Saad, Sehmi, Aymen Ben Hammadi, and Fayrouz Haddad. (2021). "An Ultra-Compact Multi-Band VCO Achieving– 196 dB FoM A with Single-Ended Tunable Active Inductor." *BioNanoScience*, 11(2), 390-400.
- [16] Jaikla, Winai, Sirigul Bunrueangsak, Fabian Khateb, Tomasz Kulej, Peerawut Suwanjan, and Piya Supavarasuwat. (2021). "Inductance Simulators and Their Application to the 4th Order Elliptic Lowpass Ladder Filter Using CMOS VD-DIBAs." *Electronics*, 10(6), 1-30, 684.
- [17] Wijenayake, Chamith, Arjuna Madanayake, Leonid Belostotski, Yongsheng Xu, and Len Bruton. (2014). "All-pass filter-based 2-D IIR filter-enhanced beamformers for AESA receivers." *IEEE Transactions on Circuits and Systems*, 61(5), 1331-1342.

- [18] Osuch, Piotr Jan, and Tinus Stander. (2018). "High-Q second-order all-pass delay network in CMOS." *IET Circuits, Devices & Systems*, 13(2), 153-162.
- [19] Yuce, Erkan, Leila Safari, Shahram Minaei, Giuseppe Ferri, and Vincenzo Stornelli. (2020). "New mixed-mode second-generation voltage conveyor based first-order all-pass filter." *IET Circuits, Devices & Systems*, 14(6), 901-907.
- [20] Elamien, Mohamed B., Brent J. Maundy, Leonid Belostotski, and Ahmed S. Elwakil. (2020). "Synthesis of Wideband High-Quality Factor Delay-Tunable Fully Differential All-Pass Filters." *IEEE Transactions on Microwave Theory and Techniques*, 68(10), 4348-4360.
- [21] Yuce, Erkan, Leila Safari, Shahram Minaei, Giuseppe Ferri, Gianluca Barile, and Vincenzo Stornelli. (2021). "A New Simulated Inductor with Reduced Series Resistor Using a Single VCII±." *Electronics*, 10(14), 1-15, 1693.
- [22] Mehra, Rishab, Vikash Kumar, and Aminul Islam. (2018). "Reliable and Q-Enhanced Floating Active Inductors and Their Application in RF Bandpass Filters." *IEEE Access*, 6, 48181-48194.
- [23] Kia, Hojjat Babaei, and Abu Khari A'ain. (2013). "A single-to-differential LNA using differential active inductor for GPS applications." *Frequenz*, 67(1-2), 27-34.
- [24] Momen, Hadi Ghasemzadeh, Metin Yazgi, and Ramazan Kopru. (2015). "Designing a new high Q fully CMOS tunable floating active inductor based on modified tunable grounded active inductor." *9th international conference on electrical and electronics engineering (ELECO)*. IEEE. 1-15.
- [25] Momen, Hadi Ghasemzadeh, Metin Yazgi, Ramazan Kopru, and Ali Naderi Saatlo. (2016). "Design of a new low loss fully CMOS tunable floating active inductor." *Analog Integrated Circuits and Signal Processing*, 89(3), 727-737.
- [26] Agrawal, Deepak, and Sudhanshu Maheshwari. (2020). "Electronically tunable grounded immittance simulators using an EX-CCCII." *International Journal of Electronics*, 107(10), 1625-1648.
- [27] Abaci, Ahmet, and Erkan Yuce. (2019). "Single DDCC based new immittance function simulators employing only grounded passive elements and their applications." *Microelectronics journal*, 83, 94-103.
- [28] Tangsrirat, Worapong. (2017). "Synthetic grounded lossy inductance simulators using single VDIBA." *IETE Journal of research*, 63(1), 134-141.

- [29] Kumar, Navnit, John Vista, and Ashish Ranjan. (2019), "A tuneable active inductor employing DXCCTA: grounded and floating operation." *Microelectronics Journal*, 90, 1-11.
- [30] Tarunkumar, Huiem, Yumnam Shantikumar Singh, and Ashish Ranjan. (2020). "An active inductor employing a new four terminal floating nullor transconductance amplifier (FTFNTA)." *International Journal of Electronics*, 107(5), 683-702.
- [31] Mamatov, Islombek, Yasin Özçelep, and Fırat Kaçar. (2022). "CNTFET based inductance simulator circuits employing single CFOA and its filter applications." *Analog Integrated Circuits and Signal Processing*, 1-8.
- [32] Dogan, Mehmet, and Erkan Yuce. (2019), "CFOA based a new grounded inductor simulator and its applications." *Microelectronics Journal*, 90, 297-305.
- [33] Yesil, Abdullah, Erkan Yuce, and Shahram Minaei. (2018). "Inverting voltage buffer based lossless grounded inductor simulators." *AEU-International Journal of Electronics and Communications*, 83, 131-137.
- [34] Jogad, Seema, Hend I. Alkhamash, Neelofer Afzal, and Sajad A. Loan. (2021). "CNTFET-based active grounded inductor using positive and negative current conveyors and applications." *International Journal of Numerical Modelling: Electronic Networks, Devices and Fields*, 34(5), e2895.
- [35] Saberhari, Alireza, Saman Ziabakhsh, Herminio Martinez, and Eduard Alarcón. (2016). "Active inductor-based tunable impedance matching network for RF power amplifier application." *Integration*, 52, 301-308.
- [36] Manjula, J., and S. Malarvizhi.(2018). "Active inductor based tunable multiband RF front end design for UWB applications." *Analog Integrated Circuits and Signal Processing*, 95(2), 195-207.
- [37] Mhiri, Mongia, Aymen Ben Hammadi, Fayrouz Haddad, Sehmi Saad, and Kamel Besbes. (2018), "Power and Noise Optimization Techniques of RF Active Inductor Using Multi-Finger Gate Transistors." *BioNanoScience*, 8(1), 264-271.

- [38] Hammadi, Aymen Ben, Mongia Mhiri, Fayrouz Haddad, Sehmi Saad, and Kamel Besbes. (2017). "An enhanced design of multi-band RF band pass filter based on tunable high-Q active inductor for nano-satellite applications." *Journal of Circuits, Systems and Computers*, 26(4), 1-20, 1750055.
- [39] Bhattacharya, Ritabrata, Ananjan Basu, and Shibani K. Koul. (2015), "A highly linear CMOS active inductor and its application in filters and power dividers." *IEEE Microwave and Wireless Components Letters*, 25(11), 715-717.
- [40] Kia, Hojjat Babaei, and Abu Khari A'ain. (2014). "A wide tuning range voltage controlled oscillator with a high tunable active inductor." *Wireless personal communications*, 79(1), 31-41.
- [41] Saad, Sehmi, Mongia Mhiri, Aymen Ben Hammadi, and Kamel Besbes. (2016) "A new low-power, high-Q, wide tunable CMOS active inductor for RF applications." *IETE journal of research*, 62(2), 265-273.
- [42] Momen, Hadi Ghasemzadeh, Metin Yazgi, and Ramazan Kopru. (2015). "A low loss, low voltage and high Q active inductor with multi-regulated cascade stage for RF applications." *2015 IEEE International Conference on Electronics, Circuits, and Systems (ICECS)*. IEEE. 149-152.
- [43] Uyanik, H. Ugur, and Nil Tarim. (2007). "Compact low voltage high-Q CMOS active inductor suitable for RF applications." *Analog integrated circuits and signal processing*, 51(3), 191-194.
- [44] Vema Krishnamurthy, Santosh, Kamal El-Sankary, and Ezz El-Masry.(2010), "Noise-cancelling CMOS active inductor and its application in RF band-pass filter design." *International Journal of Microwave Science and Technology*, 2010, 1-8.
- [45] Nair, M. U., Y. J. Zheng, and Y. Lian. (2008). "1 V, 0.18 μm -area and power efficient UWB LNA utilising active inductors." *Electronics Letters*, 44(19), 1127-1129.
- [46] Momen, Hadi Ghasemzadeh, Metin Yazgi, R. Kopru, and Ali Naderi Saatlo. (2017). "Low-loss active inductor with independently adjustable self-resonance frequency and quality factor parameters." *Integration*, 58, 22-26.
- [47] Saberkari, Alireza, Sh Kazemi, Vahideh Shirmohammadli, and Mustapha CE Yagoub. (2016). "gm-boosted flat gain UWB low noise amplifier with active inductor-based input matching network." *Integration* 52, 323-333.

- [48] Aghazadeh, Seyed Rasoul, Herminio Martinez, Alireza Saberkari, and Eduard Alarcon. (2019). "Tunable active inductor-based second-order all-pass filter as a time delay cell for multi-GHz operation." *Circuits, Systems, and Signal Processing*, 38(8), 3644-3660.
- [49] Chen, Yang, and Wenyuan Li. (2017). "An ultra-wideband pico-second true-time-delay circuit with differential tunable active inductor." *Analog Integrated Circuits and Signal Processing*, 91(1), 9-19.
- [50] Kumar, Pradeep, Ali Umit Keskin, and Kirat Pal. (2007). "Wide-band resistorless all-pass sections with single element tuning." *International Journal of Electronics*, 94(6), 597-604.
- [51] Faruqe, Omar, Aniqah Ibnat Lim, and Md Tawfiq Amin. (2020). "Tunable active inductor based VCO and BPF in a single integrated design for wireless applications in 90 nm CMOS process." *Engineering Reports*, 2(8), 1-21, e12220.
- [52] Faruqe, Omar, and Md Tawfiq Amin. (2020). "Design and Performance Analysis of Active Inductor Based VCO for IEEE 802.11 a/b/g/n/ac Applications." *International Journal of Electronics*, 107(3), 494-511.
- [53] Roobert, A. Andrew, and D. Gracia Nirmala Rani. (2021). "Design and analysis of a sleep and wake-up CMOS low noise amplifier for 5G applications." *Telecommunication Systems*, 76(3), 461-470.
- [54] Zhang, Jingzhi, Yixuan Cheng, Chenxi Zhao, Yunqiu Wu, and Kai Kang. (2018). "Analysis and design of ultra-wideband mm-wave injection-locked frequency dividers using transformer-based high-order resonators." *IEEE Journal of Solid-State Circuits*, 53(8), 2177-2189.
- [55] Kazan, Oguz, Onur Memioglu, Fatih Kocer, Adnan Gundel, and Canan Toker. (2019). "A Lumped-Element Wideband 3-dB Quadrature Hybrid." *IEEE Microwave and Wireless Components Letters*, 29(6), 385-387.
- [56] Momen, Hadi Ghasemzadeh, Metin Yazgi, R. Kopru, and A. Naderi Saatlo. (2017). "An accurate CMOS interface small capacitance variation sensing circuit for capacitive sensor applications." *Circuits, Systems, and Signal Processing*, 36(12), 4908-4918.

- [57] Faruqe, Omar, and Md Tawfiq Amin. (2019). "Wide Tuning Range Varactorless Tunable Active Inductor-Based Voltage Controlled Oscillator for Wireless Applications." *Journal of Circuits, Systems and Computers*, 28(14), 1-15, 1950242.
- [58] Elamien, Mohamed B., Brent J. Maundy, Leonid Belostotski, and Ahmed S. Elwakil. (2020). "Wideband third-order single-transistor all-pass filter." *International Journal of Circuit Theory and Applications*, 48(7), 1201-1208.
- [59] Nandi, Rabindranath, Koushick Mathur, and Sandhya Pattanayak. (2016). "Single-CFA first-order allpass filter." *IEICE Electronics Express*, 13(4), 1-8, 20151039.
- [60] Maheshwari, Sudhanshu. (2018). "Some analog filters of reduced complexity with shelving and multifunctional characteristics." *Journal of Circuits, Systems and Computers*, 27(10), 1-19, 1850150.
- [61] Herencsar, Norbert, Jaroslav Koton, Jan Jerabek, Kamil Vrba, and Oguzhan Cicekoglu. (2011). "Voltage-mode all-pass filters using universal voltage conveyor and MOSFET-based electronic resistors." *Radioengineering*, 20(1), 10-18.
- [62] Channumsin, Orapin, and Worapong Tangsrirat. (2017). "Single VDBA-based phase shifter with low output impedance." *14th International Conference on Electrical Engineering/Electronics, Computer, Telecommunications and Information Technology (ECTI-CON)*. IEEE. 427-430.
- [63] Metin, Bilgin, Kirat Pal, and Oguzhan Cicekoglu. (2011). "All-pass filters using DDCC-and MOSFET-based electronic resistor." *International Journal of Circuit Theory and Applications*, 39(8), 881-891.
- [64] Yuce, Erkan, Rakesh Verma, Neeta Pandey, and Shahram Minaei. (2019). "New CFOA-based first-order all-pass filters and their applications." *AEU-International Journal of Electronics and Communications*, 103, 57-63.
- [65] Chhabra, Jitender, Jitendra Mohan, and Bhartendu Chaturvedi. (2020). "All-Pass Frequency Selective Structures: Application for Analog Domain." *Journal of Circuits, Systems and Computers*, 30(8), 1-23, 2150152.
- [66] Kumar, Ashok, and Sajal K. Paul. (2016). "Cascadable voltage-mode all-pass filter with single DXCCII and grounded capacitor." *International Conference*

- on Microelectronics, Computing and Communications (MicroCom). IEEE.* 1-4.
- [67] Metin, Bilgin, and Kirat Pal. (2010). "New all-pass filter circuit compensating for C-CDBA non-idealities." *Journal of Circuits, Systems, and Computers*, 19(02), 381-391.
- [68] Kumngern, Montree, Jirasak Chanwutitum, and Kobchai Dejhan. (2008) "Electronically tunable voltage-mode all-pass filter using simple CMOS OTAs." *2008 International Symposium on Communications and Information Technologies. IEEE.* 1-5.
- [69] Jaikla, Winai, Pruedchawat Talabthong, Surapong Siripongdee, Piya Supavarasuwat, Peerawut Suwanjan, and Amornchai Chaichana. (2019). "Electronically controlled voltage mode first order multifunction filter using low-voltage low-power bulk-driven OTAs." *Microelectronics Journal*, 91, 22-35.
- [70] Yuce, Erkan, and Shahram Minaei. (2010). "A novel phase shifter using two NMOS transistors and passive elements." *Analog Integrated Circuits and Signal Processing*, 62(1), 77-81.
- [71] Metin, Bilgin, Norbert Herencsar, and Oguzhan Cicekoglu. (2013). "A low-voltage electronically tunable MOSFET-C voltage-mode first-order all-pass filter design." *Radioengineering*, 22(4), 985-994.
- [72] Minaei, Shahram, and Erkan Yuce. (2012). "High input impedance NMOS-based phase shifter with minimum number of passive elements." *Circuits, Systems, and Signal Processing*, 31(1), 51-60.
- [73] YÜCEL, FIRAT, and Erkan Yuce. (2016). "A new electronically tunable first-order all-pass filter using only three NMOS transistors and a capacitor." *Turkish Journal of Electrical Engineering & Computer Sciences*, 24(4), 3286-3292.
- [74] Maundy, Brent J., and Peter Aronhime. (2002), "A novel CMOS first-order all-pass filter." *International journal of electronics*, 89(9), 739-743.
- [75] Yuce, Erkan. (2010). "A novel CMOS-based voltage-mode first-order phase shifter employing a grounded capacitor." *Circuits, Systems and Signal Processing*, 29(2), 235-245.

- [76] Metin, Bilgin, and Oguzhan Cicekoglu. (2008). "Tunable all-pass filter with a single inverting voltage buffer." *2008 Ph. D. Research in Microelectronics and Electronics. IEEE.* 261-263.
- [77] Toker, Ali, and S. Özoğuz. (2003). "Tunable allpass filter for low voltage operation." *Electronics Letters*, 39(2), 175-176.
- [78] Herencsar, Norbert, Shahram Minaei, Jaroslav Koton, Erkan Yuce, and Kamil Vrba. (2013), "New resistorless and electronically tunable realization of dual-output VM all-pass filter using VDIBA." *Analog Integrated Circuits and Signal Processing*, 74(1), 141-154.
- [79] Garakoui, Seyed Kasra, Eric AM Klumperink, Bram Nauta, and Frank E. van Vliet. (2015). "Compact cascadable gm-C all-pass true time delay cell with reduced delay variation over frequency." *IEEE Journal of Solid-State Circuits*, 50(3), 693-703.
- [80] Aghazadeh, Seyed Rasoul, Herminio Martinez, and Alireza Saberkari. (2019). "5GHz CMOS all-pass filter-based true time delay cell." *Electronics*, 8(1), 1-10, 16.
- [81] Yildiz, Hacer A., Serdar Ozoguz, Ali Toker, and Oguzhan Cicekoglu. (2013). "On the realization of MOS-only allpass filters." *Circuits, Systems, and Signal Processing*, 32(3), 1455-1465.
- [82] Yıldız, Hacer A., Ali Toker, Ahmed S. Elwakil, and Serdar Ozoguz. (2014). "MOS-only allpass filters with extended operating frequency range." *Analog Integrated Circuits and Signal Processing*, 81(1), 17-22.
- [83] Metin, Bilgin, Emre Arslan, Norbert Herencsar, and Oguzhan Cicekoglu. (2011). "Voltage-mode MOS-only all-pass filter." *34th International Conference on Telecommunications and Signal Processing (TSP). IEEE.* 317-318.
- [84] Yıldız, Hacer Atar, Ali Toker, Selçuk Kılınç, and Serdar Ozoguz. (2016). "Low frequency active only filters with small chip area." *Analog Integrated Circuits and Signal Processing*, 89(3), 739-747.
- [85] Elamien, Mohamed B., Brent J. Maundy, Leonid Belostotski, and Ahmed S. Elwakil. (2019). "Single-transistor second-order allpass filters." *62nd International Midwest Symposium on Circuits and Systems (MWSCAS). IEEE.* 369-372.

- [86] Maundy, Brent J., Ahmed S. Elwakil, Leonid Belostotski, and Norbert Herencsar. (2019). "Single transistor RC-only second-order allpass filters." *International Journal of Circuit Theory and Applications*, 48(2), 162-169.
- [87] Faseehuddin, Mohammad, Jahariah Sampe, Sadia Shireen, and Sawal Hamid Md Ali. (2020). "Minimum component all pass filters using a new versatile active element." *Journal of Circuits, Systems and Computers*, 29(5), 1-31, 2050078.
- [88] Choudhary, Veena, and Anju Gupta. (2011). "Polymer/carbon nanotube nanocomposites." *Carbon nanotubes-polymer nanocomposites*, 10.5772/18423, 65-90.
- [89] Zanjani, S. Mohammad Ali, Massoud Dousti, and Mehdi Dolatshahi. (2019). "A new low-power, universal, multi-mode Gm-C filter in CNTFET technology." *Microelectronics Journal*, 90, 342-352.
- [90] Mamatov, Islombek, Yasin Özçelep, and Fırat Kaçar. (2022). "CNTFET based voltage differencing current conveyor low power and universal filter." *Analog Integrated Circuits and Signal Processing*, 110(1), 127-137.
- [91] Sayed, Shimaa Ibrahim, Mostafa Mamdouh Abutaleb, and Zaki Bassuoni Nossair. (2016). "Optimization of CNFET parameters for high performance digital circuits." *Advances in Materials Science and Engineering*, 1-10, 6303725.
- [92] Sun, Yanan, and Volkan Kursun. (2011). "N-type carbon-nanotube MOSFET device profile optimization for very large scale integration." *Transactions on Electrical and Electronic Materials*, 12(2), 43-50.
- [93] Saberkari, Alireza, Omid Khorgami, Javad Bagheri, Morgan Madec, Seyed Mohsen Hosseini-Golgoo, and Eduard Alarcón-Cot. (2018). "Design of Broadband CNFET LNA Based on Extracted I-V Closed-Form Equation." *IEEE Transactions on Nanotechnology*, 17(4), 731-742.
- [94] Patil, Nishant, Albert Lin, Edward R. Myers, Kounghmin Ryu, Alexander Badmaev, Chongwu Zhou, H-S. Philip Wong, and Subhasish Mitra. (2009). "Wafer-scale growth and transfer of aligned single-walled carbon nanotubes." *IEEE Transactions on Nanotechnology*, 8(4), 498-504.
- [95] Jin, Sung Hun, Simon N. Dunham, Jizhou Song, Xu Xie, Ji-Hun Kim, Chaofeng Lu, Ahmad Islam et al. (2013). "Using nanoscale thermocapillary

- flows to create arrays of purely semiconducting single-walled carbon nanotubes." *Nature nanotechnology*, 8(5), 347-355.
- [96] Patil, Nishant, Jie Deng, Subhasish Mitra, and H-S. Philip Wong. (2008). "Circuit-level performance benchmarking and scalability analysis of carbon nanotube transistor circuits." *IEEE Transactions on Nanotechnology*, 8(1), 37-45.
- [97] Franklin, Aaron D., Mathieu Luisier, Shu-Jen Han, George Tulevski, Chris M. Breslin, Lynne Gignac, Mark S. Lundstrom, and Wilfried Haensch. (2012). "Sub-10 nm carbon nanotube transistor." *Nano letters*, 12(2), 758-762.
- [98] Taghavi, A., C. Carta, F. Ellinger, M. Haferlach, M. Claus, and M. Schroter. (2015). "A CNTFET amplifier with 5.6 dB gain operating at 460–590 MHz." *International Microwave and Optoelectronics Conference (IMOC), IEEE*. 1-4.
- [99] Khorram, Hamidreza Ghanbari, and Alireza Kokabi. (2020). "Proposed 3.5 μ W CNTFET-MOSFET hybrid CSVCO for power-efficient gigahertz applications." *Circuit World*, 46(3), 193-202.
- [100] Jooq, Mohammad Khaleqi Qaleh, Ali Mir, Sattar Mirzakuchaki, and Ali Farmani. (2020). "Design and performance analysis of wrap-gate CNTFET-based ring oscillators for IoT applications." *Integration*, 70, 116-125.
- [101] Steiner, Mathias, Michael Engel, Yu-Ming Lin, Yanqing Wu, Keith Jenkins, Damon B. Farmer, Jefford J. Humes et al. (2012). "High-frequency performance of scaled carbon nanotube array field-effect transistors." *Applied Physics Letters*, 101(5), 1-4, 053123.
- [102] Taghavi, A., C. Carta, T. Meister, F. Ellinger, M. Claus, and M. Schroter. (2017). "A CNTFET oscillator at 461 MHz." *IEEE Microwave and Wireless Components Letters*, 27(6), 578-580.
- [103] Brady, Gerald J., Yongho Joo, Meng-Yin Wu, Matthew J. Shea, Padma Gopalan, and Michael S. Arnold. (2014). "Polyfluorene-sorted, carbon nanotube array field-effect transistors with increased current density and high on/off ratio." *ACS nano*, 8(11), 11614-11621.
- [104] Zou, Jianping, and Qing Zhang. (2021). "Advances and Frontiers in Single-Walled Carbon Nanotube Electronics." *Advanced Science*, 8(23), 1-19, 2102860.

- [105] Deng, Jie, and H-S. Philip Wong. (2007). "A compact SPICE model for carbon-nanotube field-effect transistors including nonidealities and its application—Part II: Full device model and circuit performance benchmarking." *IEEE Transactions on Electron Devices*, 54(12), 3195-3205.
- [106] Zheng, You, and Carlos E. Saavedra. (2008). "Feedforward-regulated cascode OTA for gigahertz applications." *IEEE Transactions on Circuits and System*, 55(11), 3373-3382.
- [107] Yuce, Erkan, Shahram Minaei, Norbert Herencsar, and Jaroslav Koton. (2013). "Realization of first-order current-mode filters with low number of MOS transistors." *Journal of Circuits, Systems and Computers*, 22(01), 1-14, 1250071.
- [108] Avignon-Meseldzija, Emilie, Thomas Lepetit, Pietro Maris Ferreira, and Fabrice Boust. (2017). "Negative inductance circuits for metamaterial bandwidth enhancement." *EPJ Applied Metamaterials*, 4(11), 1-13.
- [109] Zhuo, Wei, Xiaoyong Li, Sudip Shekhar, Sherif HK Embabi, José Pineda de Gyvez, David J. Allstot, and Edgar Sanchez-Sinencio. (2005). "A capacitor cross-coupled common-gate low-noise amplifier." *IEEE Transactions on Circuits and Systems II: Express Briefs*, 52(12), 875-879.
- [110] Liscidini, Antonio, Brandolini Massimo, Sanzogni Davide, Castello Rinaldo. (2006). "A 0.13 um CMOS front-end, for DCS1800/UMTS/802.11 bg with multiband positive feedback low-noise amplifier." *IEEE Journal of Solid-State Circuits*, 41(4), 981-989.
- [111] Rossi, Paolo, Antonio Liscidini, Massimo Brandolini, and Francesco Svelto. (2005). "A variable gain RF front-end, based on a voltage-voltage feedback LNA, for multistandard applications." *IEEE journal of Solid-State circuits*, 40(3), 690-697.
- [112] Woo, Sanghyun, Woonyun Kim, Chang-Ho Lee, Kyutae Lim, and Joy Laskar (2009). "A 3.6 mW differential common-gate CMOS LNA with positive-negative feedback." *2009 IEEE International Solid-State Circuits Conference-Digest of Technical Papers. IEEE*. 218-219.
- [113] Kim, Jusung, Sebastian Hoyos, and Jose Silva-Martinez. (2010). "Wideband common-gate CMOS LNA employing dual negative feedback with simultaneous noise, gain, and bandwidth optimization." *IEEE Transactions on microwave theory and techniques*, 58(8), 2340-2351.

LIST OF PUBLICATIONS

- [1] **Muhammad I. Masud**, Abu Khari Bin A'ain, Iqbal A. Khan, and Nasir Shaikh-Husin. (2019). "A CNTFET-C first order all pass filter." *Analog Integrated Circuits and Signal Processing*, 100(2), 257-268. (ISI Index, IF 1.337).
- [2] **Muhammad I. Masud**, Abu Khari Bin A'ain, Iqbal A. Khan, and Nasir Shaikh-Husin. (2019). "Design of Voltage Mode Electronically Tunable First Order All Pass Filter in ± 0.7 V 16 nm CNFET Technology." *Electronics*, 8(1), 95. (ISI Index, IF 2.397).
- [3] **Muhammad I. Masud**, Abu Khari Bin A'ain, Iqbal A. Khan, and Nasir Shaikh-Husin. (2021). "CNTFET based Voltage Mode MISO Active only Biquadratic Filter for Multi-GHz Frequency Applications." *Circuits, Systems, and Signal Processing*, 40, 1-20. (ISI Index, IF 2.225).
- [4] **M. I. Masud**, Nasir Shaikh-Husin, I. A. Khan, and A. K. Bin A'ain. (2022). "CNTFET based grounded active inductor for broadband applications." *Computers, Materials & Continua*, 73(1), 2135-2149. (ISI Index, IF 3.772).
- [5] **Masud, M. I.**, Abu Khari Bin A'ain, and Iqbal A. Khan. (2017). "Reconfigurable CNTFET based fully differential first order multifunctional filter." *2017 International Conference on Multimedia, Signal Processing and Communication Technologies (IMPACT). IEEE*. 55-59.
- [6] **Masud, M. I.**, Abu Khari Bin A'ain, and Iqbal A. Khan. (2017). "CNFET based reconfigurable first order filter." *2017 9th IEEE-GCC Conference and Exhibition (GCCCE). IEEE*. 1-9.